Effects of weak noise on oscillating flows: Linking quality factor, Floquet modes, and Koopman spectrum

Shervin Bagheri

Citation: Physics of Fluids (1994-present) **26**, 094104 (2014); doi: 10.1063/1.4895898
View online: http://dx.doi.org/10.1063/1.4895898
View Table of Contents: http://scitation.aip.org/content/aip/journal/pof2/26/9?ver=pdfcov
Published by the AIP Publishing

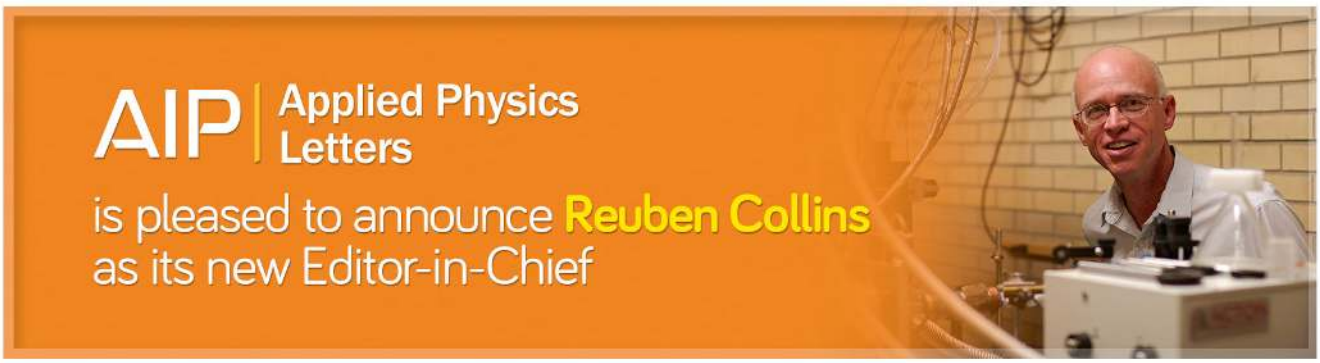

PHYSICS OF FLUIDS **26**, 094104 (2014)

Effects of weak noise on oscillating flows: Linking quality factor, Floquet modes, and Koopman spectrum

Shervin Bagheri[a)]
Linné Flow Centre, KTH Mechanics, S-100 44 Stockholm, Sweden

(Received 21 January 2014; accepted 27 August 2014; published online 22 September 2014)

Many fluid flows, such as bluff body wakes, exhibit stable self-sustained oscillations for a wide range of parameters. Here we study the effect of weak noise on such flows. In the presence of noise, a flow with self-sustained oscillations is characterized not only by its period, but also by the quality factor. This measure gives an estimation of the number of oscillations over which periodicity is maintained. Using a recent theory [P. Gaspard, J. Stat. Phys. **106**, 57 (2002)], we report on two observations. First, for weak noise the quality factor can be approximated using a linear Floquet analysis of the deterministic system; its size is inversely proportional to the inner-product between first direct and adjoint Floquet vectors. Second, the quality factor can readily be observed from the spectrum of evolution operators. This has consequences for Koopman/Dynamic mode decomposition analyses, which extract coherent structures associated with different frequencies from numerical or experimental flows. In particular, the presence of noise induces a damping on the eigenvalues, which increases quadratically with the frequency and linearly with the noise amplitude. © *2014 AIP Publishing LLC*. [http://dx.doi.org/10.1063/1.4895898]

I. INTRODUCTION

Some form of noise is always present in both numerical and laboratory experiments, and it is important to be able to quantify and control its effects on a physical fluid system. When a flow is dominated by a periodic event, such as vortex shedding behind a bluff body[1] or acoustic oscillations in an unstable combustor,[2] the periodicity of the flow oscillations may be significantly effected by very weak background noise. In the absence of noise, the state of an oscillator returns exactly to its starting position after a period $T = 2\pi/\omega$. However, in presence of noise, the trajectory fluctuates around the deterministic limit cycle and we may have other periodic solutions because after one period of oscillation the state does not return exactly to its initial position. As a consequence, the oscillations will be uncorrelated after some time, a phenomenon called *phase diffusion*. In particular, for small-amplitude noise, the time-correlation of the state decays at an exponential rate $1/\tau$. A noisy limit cycle is therefore characterized by the two time scales T and τ, which are related to each other by a measure called *the quality factor*

$$Q = 2\pi \frac{\tau}{T}. \tag{1}$$

This quantity estimates of the number of oscillations over which periodicity is maintained. When Q is very large, the oscillator is able to "keep the time," i.e., the effects of noise are not very significant. When Q is small on the other hand, the oscillations will be uncorrelated after some time.

Phase diffusion has been reported before; for example, in the experimental investigation of the effects of noise on thermoacoustic systems[2,3] (in Lieuwen,[3] a phase drift of 45° was observed after hundred cycles when the system was subject to noise). What has not been revealed before for fluid systems is that this phenomenon depends—besides on the noise amplitude and limit cycle

[a)]Electronic mail: shervin@mech.kth.se

period—on the degree of non-normality[4] of the linearized and deterministic Floquet system. As we show herein and first derived in Gaspard,[5]

$$Q \approx \frac{T^2}{\pi\epsilon}\frac{1}{|S|}, \tag{2}$$

where S is the "sensitivity" to white Gaussian noise of amplitude $\epsilon \ll 1$. It can be shown[5] that the expression for S is given by

$$S = -\frac{\mathbf{f}_1^T \tilde{\mathbf{u}}(T)}{\mathbf{f}_1^T \mathbf{e}_1}, \tag{3}$$

where $\tilde{\mathbf{u}}(T)$ is obtained by integrating the linearized equations (presented in Sec. III C). The vectors $\mathbf{f}_1$ and $\mathbf{e}_1$ are the first left (i.e., adjoint) and right eigenvectors of the linearized Floquet system. In particular, if the system is highly non-normal then $\mathbf{f}_1^T\mathbf{e}_1 \ll 1$, giving $S \gg 1$, e.g., a very large sensitivity of the limit cycle period to noise. Thus, although phase diffusion is a stochastic effect observed in the nonlinear system, Q is directly dependent on the local linear stability properties of the deterministic limit cycle. This suggests that some oscillators may in fact be very sensitive to external fluctuations, despite the common viewpoint that oscillators are "insensitive" to small amplitude external forcing (in contrast to noise amplifiers).[6]

The second objective of this paper is to use the presented theory to show the effects of weak noise on the spectrum of the Koopman operator.[7,8] This linear operator describes the evolution of observables and provides a full description of nonlinear dynamics. In Figure 1, the spectrum of the operator for an oscillator is shown in the absence (square symbols/red) and presence (circles/black symbols) of noise. In the former case, the eigenvalues are integer multiples of the fundamental frequency, i.e.,

$$\lambda_m = im\omega,$$

where $m = 0, \pm1, \pm2, \ldots$. As shown in Bagheri,[9] these Koopman eigenvalues[10] can be computed using the dynamic mode decomposition (DMD) algorithm.[11] The eigenvalues correspond to global modes, characterizing the different harmonics of the oscillating flow. In the presence of noise however, the eigenvalues can be approximated by

$$\lambda_m = im\omega - \epsilon\frac{|S|}{2T}\omega^2 m^2 + \mathcal{O}(\epsilon^2), \tag{4}$$

where S was defined in (3). For a noisy dynamical system containing a limit cycle, the spectrum (at the leading order) given by (4) becomes damped, i.e., the eigenvalues have a nonzero real part, which is proportional to the sensitivity S and increases quadratically with higher harmonics of ω. Since any experiment—numerical or laboratory—is subject to some level of random perturbations, we may—in practice—expect damped Koopman eigenvalues more often than eigenvalues on the imaginary axis (or on the unit circle). Thus, in the presence of noise one should observe parabolic shapes in the spectrum, which happens to be the form of many DMD spectra in literature.[12,13] The reason for damped eigenvalues is that the Koopman operator—which in the absence of noise is linear advection operator—becomes a linear advection-diffusion operator in the presence of noise.

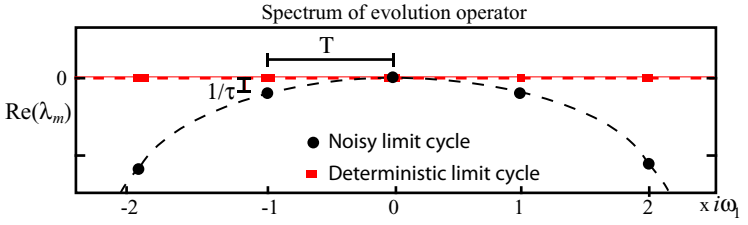

FIG. 1. Koopman eigenvalues λ_m of an oscillator with period $T = 2\pi/\omega_1$ in the presence and absence of noise.

The DMD algorithm has already established itself as a post-processing tool in the fluids community, but the contributed work on its theoretical basis, mathematical aspects as well as the physical significance of the output of the algorithm have been few.[9,10,14–16] The reason for the rapid success of the method is its many advantages over both discrete Fourier decomposition (DFT) and Proper orthogonal decomposition (POD); it does not require the self-sustained frequencies to be known by the user, and it can even provide a growth/decay rate to each mode, i.e., the frequency is complex. On the other hand, its main disadvantage is that the method is sensitive to noise-contaminated data.[17] An understanding of the phase diffusion phenomenon provides a simple explanation for the noise sensitivity of the algorithm.[11] For oscillating flows that are subject to very small noise, discrete samples of one realization may result in an output of DMD that is not unique, since each realization has a slightly different period (due to phase diffusion). Instead, by using observables based on a collection of trajectories (e.g., statistics), a unique and robust set of DMD eigenvalues should emerge. Moreover, for an oscillator, the leading eigenvalue should have a decay rate that can be associated with the quality factor Q.

The paper is organized as follows. In Sec. II, we provide a general formulation of noisy oscillators and provide specific examples on the Stuart-Landau equation. In particular, we show that a noisy limit cycle can be characterized by two time scales and that these times scales are captured in the spectrum of evolution operators. Using computations, we show how the spectrum pertaining to the limit cycle depends on the noise amplitude and on the frequency of the limit cycle. Finally, the resemblance of the computed spectrum with a DMD spectrum from literature is discussed. In Sec. III, we present the essential theory of Gaspard[5] in a simplified form. The spectrum of a limit cycle in the presence of weak noise is derived analytically and compared to the computed spectrum in Sec. II. Moreover, this section shows how the sensitivity of the limit cycle to phase diffusion depends on local linear analysis, and interprets this fact in the context of hydrodynamic stability theory. Finally in the Appendix, we provide a short note relating the current work to the structural sensitivity analysis of earlier work.[18]

II. NOISY OSCILLATORS

A. Evolution of the state

Consider a nonlinear system subject to m stochastic excitations,

$$\frac{\partial \mathbf{u}}{\partial t} = \mathbf{f}(\mathbf{u}) + \sqrt{\epsilon}\sum_{k=1}^{m} \mathbf{g}_k(\mathbf{u})\hat{\xi}_k(t), \tag{5}$$

where $\mathbf{u} \in \mathbb{R}^n$ is the flow field (or state) and $\mathbf{f}(\mathbf{u})$ represents the discretized right-hand side of the Navier-Stokes equations. We assume that the vector fields $\mathbf{f}(\mathbf{u})$ and $\mathbf{g}_k(\mathbf{u})$ do not depend explicitly on time. Moreover, ϵ is the forcing amplitude and $\hat{\xi}_k(t)$ is assumed to be a Gaussian white noise, satisfying

$$\langle \hat{\xi}_k(t) \rangle = 0, \qquad \langle \hat{\xi}_k(t)\hat{\xi}_l(t') \rangle = \delta_{kl}\delta(t-t'),$$

where $k, l = 1, \ldots, m$ and the angled brackets denote the mean value. We define the time-forward mapping Φ^t by $\mathbf{u}(t) = \Phi^t \mathbf{u}_0$, which provides the deterministic flow at time t issued from the initial flow field $\mathbf{u}_0$—essentially a Navier-Stokes solver. We assume that the deterministic system ($\epsilon = 0$) contains a limit cycle[19] of period T, i.e.,

$$\mathbf{u}_s = \Phi^{kT}\mathbf{u}_s, \qquad k = 0, \pm 1, \pm 2, \ldots,$$

where $\mathbf{u}_s$ is a point on the limit cycle.

In this paper, we will illustrate the effect of weak noise on a simpler system than the Navier-Stokes equations. Close to the critical threshold for Hopf bifurcation (e.g., $Re \approx 50$ for a cylinder flow), the state evolves in a slow one-dimensional center manifold and can be described by a complex amplitude $z(t)$ that satisfies the Stuart-Landau (SL) equation. In the presence of noise, the SL equation

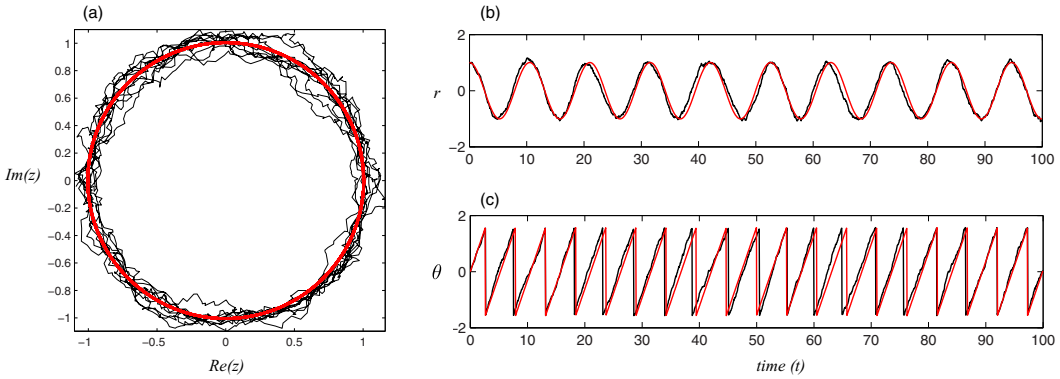

FIG. 2. In (a) the limit cycle is shown in state-space (z). In (b) and (c), the time evolution of the amplitude (r) and the phase (θ) of the state are shown, respectively. The gray line (red) shows the deterministic limit cycle, whereas the black line shows a noisy limit cycle. Parameters for (6) are $\mu = 1$, $\beta = 0.3$, $\gamma = 0.9$, and $\epsilon = 0.01$.

reads

$$\frac{\partial z}{\partial t} = (\mu + i\gamma)z - (1 + i\beta)|z|^2 z + \sqrt{\epsilon}\hat{\eta}, \tag{6}$$

where $\epsilon \ll 1$ is the amplitude of the Gaussian white stochastic term $\hat{\eta}(t)$ (with zero mean and unit variance). In Secs. II B and II C, it will be more convenient to work with the SL equation (6) in polar coordinates $z(t) = r(t)\exp(i\theta(t))$,

$$\frac{\partial r}{\partial t} = \mu r - r^3 + \sqrt{\epsilon}\left[\cos(\theta)\hat{\eta}_r + \sin(\theta)\hat{\eta}_i\right], \tag{7}$$

$$\frac{\partial \theta}{\partial t} = \gamma - \beta r^2 + \frac{\sqrt{\epsilon}}{r}\left[-\sin(\theta)\hat{\eta}_r + \cos(\theta)\hat{\eta}_i\right], \tag{8}$$

where $\hat{\eta} = \hat{\eta}_r + i\hat{\eta}_r$.

For $\mu > 0$ and in the absence of noise ($\epsilon = 0$), the state evolves on the limit cycle

$$r = \sqrt{\mu}, \qquad \theta(t + kT) = \theta(t),$$

where $k = 0, \pm 1, \pm 2, \ldots$, is the repetition number of the prime period $T = 2\pi/\omega$ and $\omega = \gamma - \mu\beta$. However, in presence of noise ($\epsilon \neq 0$), we may have other periodic solutions because after one period of oscillation the state does not return exactly to its initial position. In Figure 2(a), the deterministic (gray/red) and noisy (black line) limit cycles are compared in state space. One observes that the noisy trajectory fluctuates around the deterministic limit cycle. These noisy limit cycles represent periodic solutions with a slightly different period, $T_{\text{noise}} = T + \delta t$. Figures 2(b) and 2(c) compare the amplitude and the phase of limit cycles in the time domain, where it is evident that the main effect of noise is a drift of the phase.

Since the trajectory of a noisy cycle fluctuates randomly around the deterministic limit cycle, it is meaningful to characterize the expected value of the random state. Figure 3 shows the evolution of the expected value of the state, $\mathbb{E}[z]$, for $\epsilon = 0.01$. The expected value has oscillations of period $T = 2\pi/0.6$ (Figure 3(a)) and shows an exponential decay in time at the rate $1/\tau = -0.0054$ (Figure 3(b)). In Subsection II B, we show that these two time scales are captured in the spectrum of a linear operator.

B. Evolution of the expected value of observables

Consider an observable of the state $a(\mathbf{u})$ and define the function $v(\mathbf{u}_0, t)$ as its expectation value, i.e.,

$$v(\mathbf{u}_0, t) = \mathbb{E}\left[a(\mathbf{u}) \mid \mathbf{u}(0) = \mathbf{u}_0\right].$$

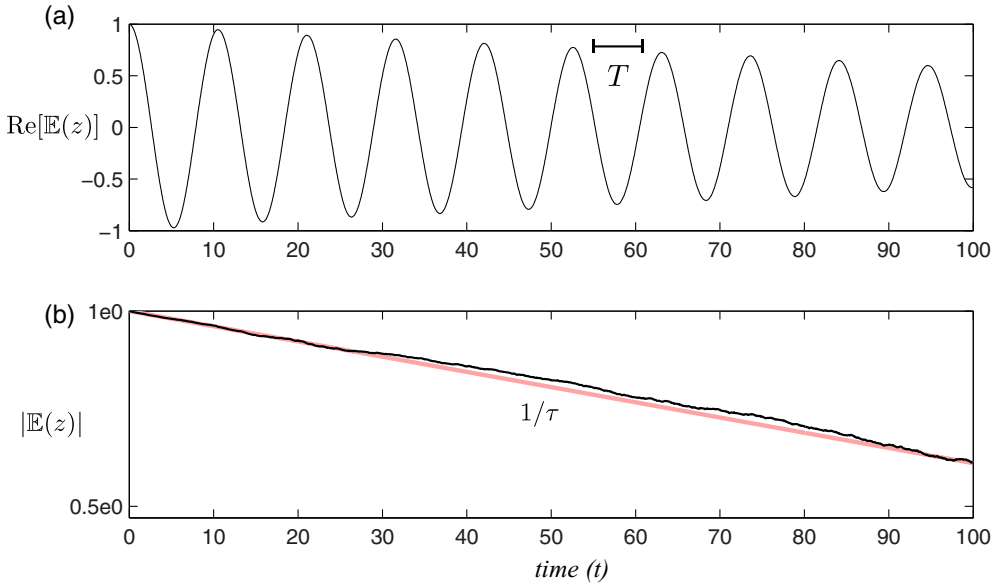

FIG. 3. Top frame (a) shows the time evolution of the real part of the expected value $\mathbb{E}[z]$ for $\epsilon = 0.01$. Black line bottom frame (b) shows that absolute value on a logarithmic scale. Gray (red) shows the exponential function with decay rate (σ_1) given by the leading eigenvalue of $\mathcal{A}$. Parameters of the SL equation are the same as in Figure 2.

Then one may show[20] that $v(\mathbf{u}, t)$ (dropping the subscript $_0$ on $\mathbf{u}$) satisfies

$$\frac{\partial v(\mathbf{u}, t)}{\partial t} = f_i(\mathbf{u})\frac{\partial}{\partial u_i}v(\mathbf{u}, t) + \epsilon Q_{ij}(\mathbf{u})\frac{\partial^2}{\partial u_i \partial u_j}v(\mathbf{u}, t) \equiv \mathcal{A}v(\mathbf{u}, t), \tag{9}$$

with $v(\mathbf{u}, 0) = a(\mathbf{u})$ and

$$Q_{ij}(\mathbf{u}) = \frac{1}{2}g_{ki}(\mathbf{u})g_{kj}(\mathbf{u})$$

is a positive-definite matrix of diffusion. Here, we have the written vector the fields $\mathbf{f}$ and $\mathbf{g}$ in (5) with a tensor notation.

Thus, whereas the time evolution of the state $\mathbf{u}(t)$ is governed by a nonlinear finite-dimensional system (5), the time evolution of the expected value of an observable function of the state $v(\mathbf{u}, t)$ is governed by a linear convection-diffusion partial differential equation (9).[21] The above PDE induces the evolution operator

$$v(\mathbf{u}, t) = e^{\mathcal{A}t}a(\mathbf{u}). \tag{10}$$

For a deterministic system ($\epsilon = 0$), the operator becomes hyperbolic with characteristics as the integral curves of (5), i.e.,

$$v(\mathbf{u}, t) = a(\Phi^t\mathbf{u}).$$

Thus, for a noise-free system, $v(\mathbf{u}_0, t)$ is the observable $a(\mathbf{u})$ evaluated on the point $\mathbf{u}(t)$ of the trajectory starting from $\mathbf{u}_0$. This is by definition the Koopman operator.[10,22] As stated earlier, in the presence of noise, $v(\mathbf{u}_0, t)$ is the expected value of the observable at the point $\mathbf{u}(t)$ of the trajectory starting from $\mathbf{u}_0$. We may thus consider the evolution operator $\exp(\mathcal{A}t)$ as the Koopman operator with respect to a noisy system.

Next, consider the spectrum of $\mathcal{A}$, which for a noisy limit cycle consists of discrete points only.[23] Let the sequence of complex numbers $\{\lambda_m\}$ be the eigenvalues of $\mathcal{A}$ and $\{\psi_m(\mathbf{u})\}$ the corresponding eigenfunctions, i.e.,

$$\mathcal{A}\psi_m = \lambda_m\psi_m,$$

where $m = 0, 1, 2, \ldots$. The expected value of an observable expanded in $\{\psi_m\}$ is then given by,

$$v(\mathbf{u}_0, t) = \sum_{m=0}^{\infty} \alpha_m e^{\lambda_m t} \psi_m(\mathbf{u}_0), \tag{11}$$

where α_m are the expansion coefficients.

1. Spectrum of SL equation

Before we derive λ_m for a general noisy oscillator, let us solve for the eigenvalues $\{\lambda_m\}$ associated with the SL equation. Equation (9) for the SL equations (7) and (8) takes the form

$$\frac{\partial v}{\partial t} = (\mu r - r^3)\frac{\partial v}{\partial r} + (\gamma - \beta r^2)\frac{\partial v}{\partial \theta} + \epsilon \left[Q_{rr}\frac{\partial^2 v}{\partial r^2} + Q_{r\theta}\frac{\partial^2 v}{\partial \theta \partial r} + Q_{\theta\theta}\frac{\partial^2 v}{\partial \theta^2} \right], \tag{12}$$

where $Q_{rr} = (\cos^2(\theta) + \sin^2(\theta) r^{-2})/2$, $Q_{r\theta} = (\sin(2\theta) - \sin(2\theta) r^{-2})/4$, and $Q_{\theta\theta} = (\cos^2(\theta) r^{-2} + \sin^2(\theta))/2$. We discretize[24] the right-hand side of (12) and solve an eigenvalue problem of the discretized operator. The global spectrum of the discretized operator is shown in Figure 4. The spectrum is global since it characterizes the entire phase-space of the nonlinear system, i.e., it is not based on a linearization around the periodic orbit. The branches marked in circles (red) are associated with the limit cycle at $r = \sqrt{\mu}$, whereas the squares (blue) are associated with the unstable equilibrium at $r = 0$.[25]

In the remaining part of this paper, we focus our attention on the leading eigenvalues inside the gray region in Figure 4(a) (shown in close-up in Figure 4(b)). The eigenvalues form a distinct parabolic branch and all are stable except one, which is on the imaginary axis ($\lambda_0 = 0$). The expected value of an observable expanded in $\{\psi_m\}$ is

$$v(r_0, \theta_0, t) = \alpha_0 \psi_0 + \alpha_1 e^{\lambda_1 t} \psi_1 + c.c. + \ldots, \tag{13}$$

where α_m are the expansion coefficients and $c.c.$ denotes complex conjugate terms. We thus observe that the expansion term corresponding to $\lambda_0 = 0$ is the asymptotic mean value of the observable and the remaining terms reflect the exponential decay towards this limit. The damped eigenvalues

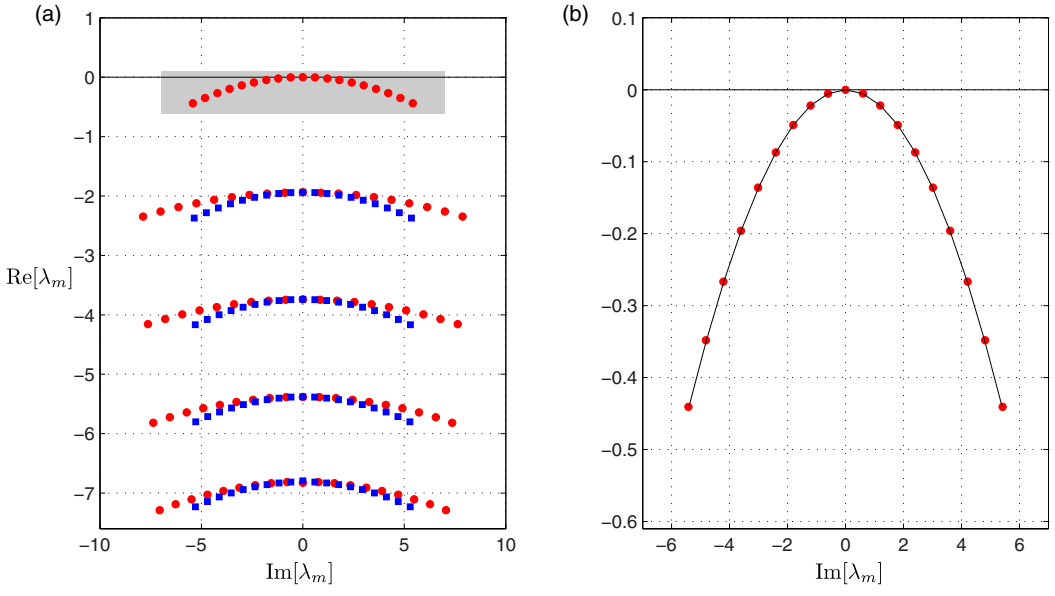

FIG. 4. Spectrum of the evolution operator $\mathcal{A}$ with respect to the SL equation. Parameters are the same as in Figure 2. Left figure (a) shows the leading 380 eigenvalues. Circles (red) and squares (blue) correspond to dynamics related to the limit cycle and the unstable fixed point, respectively. Right figure (b) shows the first branch of spectrum, where the black line is parabolic fit (Eq. (16)).

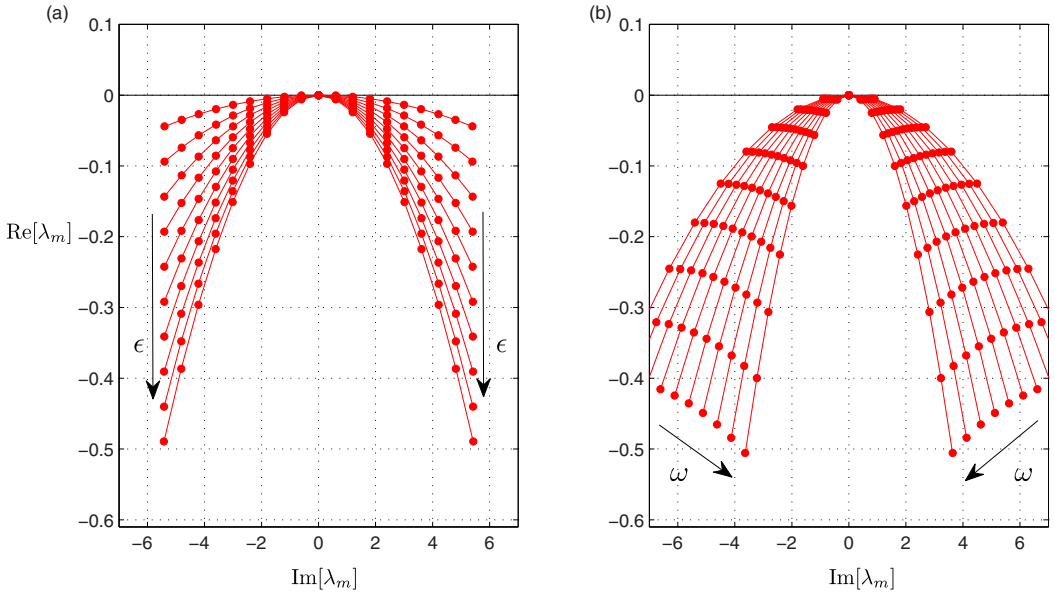

FIG. 5. First parabolic branch of the global spectrum of the SL equation corresponding to the observable dynamics of the limit cycle. Left figure (a) shows how the damping of eigenvalues increases linearly with the noise amplitude ϵ (frequencies are left unmodified). Right figure (b) shows that damping increases quadratically with a shift in limit cycle frequency β.

observed in the presence of noise are caused by the diffusion term in $\mathcal{A}$ (second-order derivative in (9)). This diffusive process is not related to the viscous diffusion of the flowing fluid. The decay is for long times dominated by the first eigenvalue

$$\lambda_1 = i\omega_1 + \sigma_1, \tag{14}$$

which for SL spectrum shown in Figure 4 has the value

$$\lambda_1 = i0.60 - 0.0054.$$

These values match the oscillations $T = 2\pi/0.6$ and the decay rate $1/\tau = -0.0054$ reported in Figure 3. We thus observe that the time scales τ and T are dominated by the real and imaginary parts of λ_1, respectively. In particular, the quality factor (1) can be approximated as

$$Q = 2\pi\frac{\tau}{T} \approx \frac{|\omega_1|}{|\sigma_1|}. \tag{15}$$

To investigate the first parabolic branch further, we vary the noise amplitude ϵ and the frequency ω of the limit cycle. We observe that the eigenvalues increase linearly with ϵ (Figure 5(a)) and quadratically with ω (Figure 5(b)). Indeed, as $\epsilon \to 0$ the parabolas approach the Koopman eigenvalues. These observations suggest that we can fit a function to the first branch of eigenvalues in the form,

$$s(\omega, \epsilon) = im\omega - \frac{\epsilon}{2}\kappa m^2\omega^2, \tag{16}$$

where $m = 0, \pm1, \pm2, \ldots$ and κ is some constant. The black line in Figure 4(b) shows the fit with a black solid line. Comparing the parabolic fit (16) of the SL equation to the formula of a general noisy oscillator (4), we observe that $\kappa = |S|/T$, where S is given by (3). This relation is derived in Sec. III.

C. Dynamic mode decomposition

As shown in Bagheri,[9] the Koopman eigenvalues of oscillators may be approximated using the DMD algorithm[11] (the algorithm is detailed in Schmid[11] and not given here). Thus, as expected,

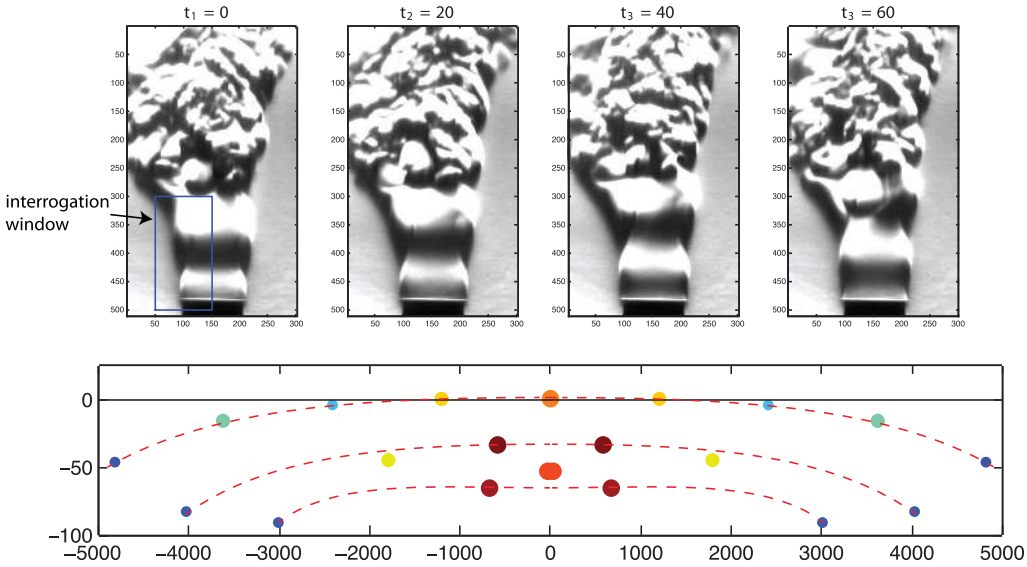

FIG. 6. The top frame shows four snapshots of a helium jet; it uses Schlieren techniques to visualize the dynamics of the fluid structure; thus, only a scalar field—proportional to the density gradient and quantified by its location on a grey-scale colormap—is being processed. The first snapshot (most left) also contains the size and location (box marked with an arrow) of the interrogation window for the subsequent DMD-analysis. Note from this snapshots that the flow is turbulent away from the nozzle, but initially shows very well structured coherent motion, that is also oscillatory in time. The bottom frame in the figure shows the spectrum extracted using the DMD algorithm. Figure taken from Schmid *et al.*[12] Reprinted with permission from P. Schmid *et al.* Copyright 2009 Springer Science and Business Media.

the eigenvalues associated with the deterministic limit cycle obtained from the DMD in Bagheri[9] where all located on the imaginary axis. However, in practice and often for experimental data, the DMD spectrum shows damped eigenvalues. We show in Figure 6 a typical DMD spectrum found in literature.[12] The spectrum shows the trait of an advection-diffusion operator, i.e., parabolic branches are clearly observed. These parabolic shapes are indeed very similar to the spectrum of a noisy limit cycle as outlined in Sec. II B. In the context of the theory presented herein, one may hypothesize that the parabolic branches observed in DMD spectra are due to the presence of noise. In that case, one would further expect that the decay rate of the first eigenvalue in the spectrum provides an estimate of the quality factor. However, whereas the parabolic shapes in the spectrum of $\mathcal{A}$ defined by (10) are related to expected values of an observable, classical DMD is often based on sampling directly the observable (not its statistics). As shown in this paper, for a noisy and nonlinear oscillator, each realization of a trajectory (even with the same initial condition) is different, and hence the DMD spectrum will vary for different realizations of the same system. One way to make the algorithm robust and the spectrum unique is to use statistical observables, such as expectation values and correlation functions. Using such a probabilistic approach, one is effectively investigating the evolution of a set of trajectories. One effort to generalize DMD to datasets based on more than one trajectory is the recent DMD theory presented in Tu *et al.*,[16] which provides Ritz vectors and values of multiple trajectories.

III. WEAK-NOISE THEORY

This section provides the necessary theory to derive Eqs. (3) and (4). In places where lengthy but rather straightforward derivations are required, we refer to other papers. This is because the key points of this paper are the consequences of weak-noise theory linking quality factor, Floquet analysis and Koopman spectrum. The main theory in a more general and rigorous form can be found in Gaspard.[5] Specifically, the structure of this section is as follows. The first part shows that Q in (1) may be approximated by the first eigenvalue λ_1 of an evolution operator. Moreover, Q depends on

the noise amplitude ϵ, the period T, and the sensitivity S. The key step is the derivation of a particular Hamilton-Jacobi equation. The associated Hamilton's equation of motion provides a deterministic nonlinear system of twice the size of the stochastic system (5). These equations describe each noisy limit cycle as a deterministic cycle in an extended phase space. The second part of this section shows expression (3), i.e., that S is composed of Floquet vectors of the linearized deterministic dynamics.

A. The Fokker-Planck operator

In this section, we turn our attention to the Fokker-Planck operator that governs the time evolution of the probability density function $\rho(\mathbf{u}, t)$.[26] For the (Ito) stochastic equation (5), it takes the form

$$\frac{\partial \rho(\mathbf{u}, t)}{\partial t} = -\frac{\partial}{\partial u_i}\left[f_i(\mathbf{u})\rho(\mathbf{u}, t)\right] + \epsilon \frac{\partial^2}{\partial u_i \partial u_j}\left[Q_{ij}(\mathbf{u})\rho(\mathbf{u}, t)\right] \equiv \mathcal{A}^\dagger \rho(\mathbf{u}, t). \tag{17}$$

Here, $\mathcal{A}^\dagger$ is the adjoint of $\mathcal{A}$ with respect to the inner-product,

$$\langle q, \rho \rangle = \int_{\mathbb{R}^n} q(\mathbf{u})\rho(\mathbf{u}) d\mathbf{u}.$$

As a consequence the two operators have the same spectrum and the eigenfunctions ($\tilde{\psi}_n$) of $\mathcal{A}^\dagger$ are bi-orthogonal to the eigenfunctions of $\mathcal{A}$ (ψ_m),

$$\langle \psi_m, \tilde{\psi}_n \rangle = \delta_{mn}.$$

For a system with a limit cycle, $\mathcal{A}^\dagger$ is stable (e.g., no eigenvalues with positive real part); this means that as time goes on, the probability density function $\rho(\mathbf{u}, t)$ will reach a stationary distribution $\rho_\infty(\mathbf{u})$, which is non-zero only in an neighborhood of the deterministic limit cycle, i.e.,

$$\lim_{t\to\infty} \rho(\mathbf{u}, t) = \rho_\infty(\mathbf{u}). \tag{18}$$

In order to find an analytical value of λ_1, we will need to consider the autocorrelation function of two observables $a(\mathbf{u})$ and $b(\mathbf{u})$ along the noisy trajectory $\mathbf{u}(t)$ (see, for example, Ch. 7 in Risken[26]),

$$C_{ab}(t) = \int a(\mathbf{u}) e^{\mathcal{A}^\dagger t} b(\mathbf{u}) \rho_\infty(\mathbf{u}) d\mathbf{u}. \tag{19}$$

Using the left and right eigenfuntions of the evolution operator as well as the invariant density, we can form a generalized expansion of the autocorrelation function

$$C_{ab}(t) = \sum_{m=0}^{\infty} \alpha_m e^{\lambda_m t} \beta_m = C_0 + C_1 e^{\lambda_1 t} + \ldots, \tag{20}$$

where $\alpha_m = \langle \tilde{\psi}_m, a \rangle$,

$$\beta_m = \int \psi_m^*(\mathbf{u}) b(\mathbf{u}) \rho_\infty(\mathbf{u}) d\mathbf{u},$$

and $C_m = \alpha_m \beta_m$. Any correlation function is thus composed of a steady term (C_0) and exponential terms C_m. In particular, the temporal behavior of the autocorrelation function is, for long times, dominated by the leading non-zero eigenvalue λ_1.

B. Quality factor in terms of first Fokker-Planck eigenvalue

In the weak-noise limit $\epsilon \to 0$, an approximation of the first eigenvalue λ_1 (14) can be found analytically. One may write[27] the density in the form

$$\rho(\mathbf{u}, t) = \exp\left(-\frac{1}{\epsilon}\phi_0(\mathbf{u}, t)\right). \tag{21}$$

Inserting the density into (17), we get

$$\frac{\partial \phi_0}{\partial t} + H(\mathbf{u}, \nabla \phi_0) = 0, \tag{22}$$

with the particular Hamiltonian[28]

$$H(\mathbf{u}, \mathbf{p}) = f_i(\mathbf{u}) p_i + Q_{ij}(\mathbf{u}) p_i p_j. \tag{23}$$

Here $\phi_0(\mathbf{u}, t)$ can be interpreted as Hamilton's principal function and $\mathbf{p}(t) = \nabla \phi_0$ as the momenta canonically conjugated to the state—or as the adjoint variable from an optimization viewpoint. To obtain the solution to (22), we may solve the associated Hamilton's equations of motion,

$$\frac{\partial u_i}{\partial t} = +\frac{\partial H}{\partial p_i} = f_i + 2Q_{ij} p_j, \tag{24}$$

$$\frac{\partial p_i}{\partial t} = -\frac{\partial H}{\partial u_i} = -\frac{\partial f_j}{\partial u_i} p_j - \frac{\partial Q_{jk}}{\partial u_i} p_j p_k. \tag{25}$$

In the weak-noise limit, we may thus approximate the stochastic system (5), with a deterministic dynamical system of twice the size. The first equation is the nonlinear Navier-Stokes equations but with a deterministic forcing term $2Q_{ij}(\mathbf{u})p_j(t)$. The second equation for $\mathbf{p}(t)$ is composed of the linearized adjoint Navier-Stokes equations and a quadratic nonlinear term. When $\mathbf{p} = 0$, Eqs. (24) and (25) reduce to the deterministic equations,

$$\frac{\partial \mathbf{u}}{\partial t} = \mathbf{f}(\mathbf{u}) \qquad \text{for} \qquad \mathbf{p} = 0.$$

When $\mathbf{p} \neq 0$, the pair of equations may be interpreted as extending the original state space to accommodate for limit cycles of slightly different periods due to the presence of weak noise. Note that the Hamiltonian form does not arise because of the mechanics of the system, but is an artifact of the leading approximation of noisy dynamics.

Moreover, H does not explicitly depend on time,

$$\frac{dH}{dt} = 0 \qquad \rightarrow \qquad H(\mathbf{u}, \mathbf{p}) = E,$$

where E is the "pseudo-energy,"[5] which is constant along trajectories of $(\mathbf{u}, \mathbf{p})$.

1. Approximation of λ_1 in the weak noise limit

Consider a point on the limit cycle $\mathbf{u}_s$ that has been reached after time kT. It can be shown (see Eq. (90) in Gaspard[5]) that the lowest non-zero term of the Taylor expansion of $\phi_0(\mathbf{u}, t)$ around $\mathbf{u}_s$ and time kT is

$$\phi_0(\mathbf{u}, t) \approx -\frac{1}{2k|S|}(t - kT)^2, \tag{26}$$

where S is

$$S = \frac{\partial T}{\partial E}.$$

It will be shown in Sec. III C that S is given by expression (3) and has the interpretation of "sensitivity" of the limit cycle to noise, since its size is determined by the degree of non-normality of the linearized system.

Inserting (26) into (21), we get an approximation of the probability density function (21) in the form

$$\rho(t) \sim \exp\left[-\frac{(t - kT)^2}{2k\epsilon|S|}\right]. \tag{27}$$

Note that this Gaussian depends only on time; it captures only the flow direction (longitudinal direction of the limit cycle). It can be shown (see Eq. 88 in Gaspard[5]) that this term dominates

over the Gaussian term in transverse component of the limit cycle time goes on. Expression (27) suggests that recurrences of the noisy system are distributed randomly around the period T of the deterministic limit cycle. In particular, we may note from (27) that

$$\text{mean}: \qquad \langle t \rangle \approx kT, \tag{28}$$

$$\text{variance}: \qquad \langle (t - kT)^2 \rangle \approx \epsilon k |S|, \tag{29}$$

which gives the following important insights:

(i): variance is proportional to noise amplitude (ϵ)
(ii): variance increases with the repetition number k
(iii): variance is proportional to the "sensitivity" $|S|$.

The first point simply asserts that the Gaussian becomes sharper with smaller noise amplitude. The second point is phase diffusion: the width of the Gaussian distribution becomes wider for each repetition. This means that for each repetition, the likelihood increases that the noisy flow returns to a position far from the point which the deterministic point would return to. The third point states that the variance—thus phase diffusion—increases with the non-normality of system $|S|$.

Consider now the auto-correlation function (19), which in the presence of weak noise has a probability function of Gaussian type according to (27). As t increases, the probability density function is composed of increasingly wider Gaussian pulses. Using a Fourier transform in time, it can be shown (see Eqs. (56)–(59) in Ref. 29) that

$$C_{ab}(t) \approx C_0 + |C_1| \exp\left(i \frac{2\pi}{T} t\right) \exp\left(-\frac{\epsilon |S|}{2T} \left(\frac{2\pi}{T}\right)^2 t\right), \tag{30}$$

where C_0 and C_1 are some constant coefficients. Comparing to (20), we can identity

$$\omega_1 = \frac{2\pi}{T} \qquad \text{and} \qquad \sigma_1 = -\frac{\epsilon |S|}{2T} \left(\frac{2\pi}{T}\right)^2. \tag{31}$$

In summary, (31) is the first eigenvalue ($m = 1$) of the more general expression (4). We observe that due to the presence of weak noise, we have a negative real part of the first eigenvalue, but the frequency is left unmodified. The reason is that the leading non-zero Taylor expansion term of ϕ_0 is quadratic, with the effect that phase diffusion results only a damping effect, and not a frequency shift.

In Table I, the real part of the leading eigenvalue σ_1 is listed for limit cycles of the SL equation with different periods. The difference between the theoretical estimate of σ_1 and the numerically approximated (see Figure 4) decay rate is $\mathcal{O}(\epsilon^2)$.

TABLE I. Comparison between theoretically estimated decay rate σ_1 and numerically computed decay rate for limit cycles of different periods T. The error between theory and computations is $\mathcal{O}(\epsilon^2)$. Moreover, the decay rate increases linearly with the sensitivity S.

T	S	σ_1 (num)	σ_1 (theory)
6.9813	8.6189	−0.0050	−0.0050
7.4406	10.4505	−0.0050	−0.0050
7.9646	12.8765	−0.0051	−0.0050
8.5680	16.1520	−0.0051	−0.0051
9.2703	20.6721	−0.0052	−0.0051
10.0980	27.0697	−0.0054	−0.0052
11.0880	36.3978	−0.0056	−0.0053
12.2932	50.4912	−0.0058	−0.0054
13.7924	72.7303	−0.0060	−0.0055
15.7080	109.6457	−0.0063	−0.0056

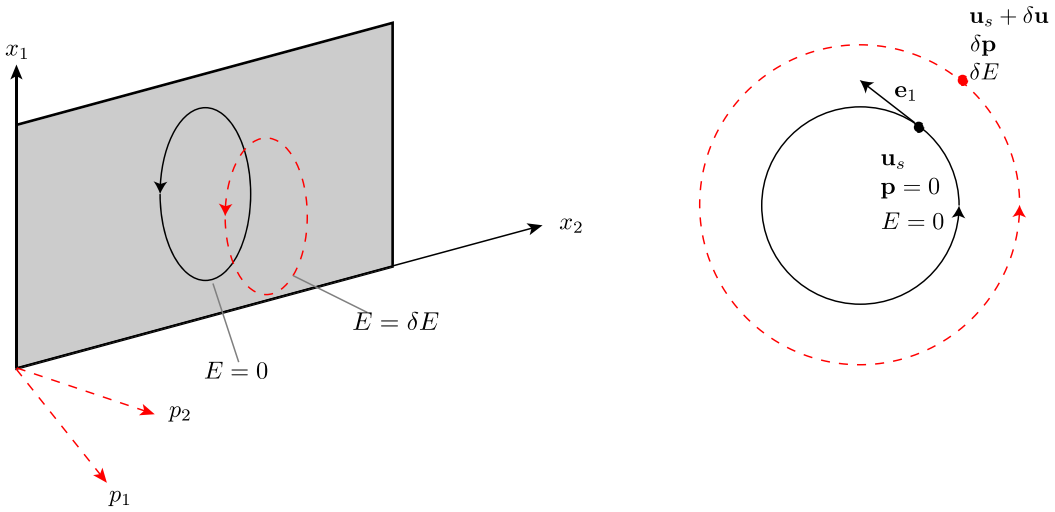

FIG. 7. The deterministic limit cycle (black) lives in the $\mathbf{p} = 0$ subspace and has zero pseudo energy. Noisy limit cycles (dashed/red) are described by extending the state space using $\mathbf{p}$ and a measure of their deviation from the deterministic cycle is given by E.

C. Quality factor in terms of Floquet eigenvectors

The pseudo energy E is constant on each noisy trajectory; it can be regarded as a measure of deviation of noisy trajectory from its deterministic prediction (see Figure 7). The derivative $\partial_E T$, written as

$$\delta T = \frac{\partial T}{\partial E}\delta E, \tag{32}$$

shows that if $\partial_E T$ is large, then a small perturbation of pseudo energy gives a large deviation of the deterministic time period. In this section, we linearize the Hamilton equations (24) and (25) around the noiseless limit cycle followed by a transformation of the system in the basis spanned by eigenvectors of the linear system. By forming the inner product with the left eigenvector we arrive at expression (3).

1. Linearized Hamilton-Jacobi equations

In order to find an explicit expression for $\partial_E T$, we consider the linearized Hamilton's equations about an arbitrary point $(\mathbf{u}, \mathbf{p})$,

$$\frac{\partial \tilde{u}_i}{\partial t} = A_{ij}\tilde{u}_j + 2Q_{ij}\tilde{p}_j, \tag{33}$$

$$\frac{\partial \tilde{p}_i}{\partial t} = -A_{ji}\tilde{p}_j, \tag{34}$$

where $A_{ij}(\mathbf{u}) = \partial f_i(\mathbf{u})/\partial u_j$ denotes the stability matrix. On the deterministic limit cycle, the stability matrix is T-periodic, i.e., $A(t) = A(\mathbf{u}(t)) = A(t+T)$. The solutions to (33) and (34) are

$$\begin{pmatrix} \tilde{\mathbf{u}}(t) \\ \tilde{\mathbf{p}}(t) \end{pmatrix} = \begin{pmatrix} M(t) & N(t) \\ 0 & M(t)^{-T} \end{pmatrix} \begin{pmatrix} \tilde{\mathbf{u}}(0) \\ \tilde{\mathbf{p}}(0) \end{pmatrix}, \tag{35}$$

where the Jacobian matrix $M(t) \in \mathbb{R}^{n\times n}$ (or the fundamental matrix) is the solution of

$$\dot{M}(t) = A(\mathbf{u})M(t), \qquad M(0) = I,$$

and $N(t) \in \mathbb{R}^{n\times n}$ is given by,

$$N(t) = 2M(t)\int_0^t M(\tau)^{-1}\mathbf{Q}(\mathbf{u})M^{-T}(\tau)\,d\tau.$$

The above equations provide the evolution of an infinitesimal displacement $(\tilde{\mathbf{u}}, \tilde{\mathbf{p}})$ along the trajectory $(\mathbf{u}, \mathbf{p})$ starting at $(\mathbf{u}_0, \mathbf{p}_0)$.

2. Expansion around noiseless limit cycle

The noiseless limit cycle of period T has zero pseudo energy ($E = 0$) and lives in the $\mathbf{p} = 0$ subspace. For the noisy cycle the following holds (see Figure 7):

$$\mathbf{u}(T + \delta T) = \mathbf{u}(0), \tag{36}$$

$$\mathbf{p}(T + \delta T) = \mathbf{p}(0), \tag{37}$$

$$E = \delta E. \tag{38}$$

We may describe (36) in terms of perturbations around the deterministic cycle,

$$\mathbf{u}_s(T + \delta T) + \tilde{\mathbf{u}}(T + \delta T) = \mathbf{u}_s(0) + \tilde{\mathbf{u}}(0), \tag{39}$$

where $\mathbf{u}_s$ is a point on the deterministic limit cycle. Taylor expanding both sides around $T + \delta T$ and using $\mathbf{u}_s(T) = \mathbf{u}_s(0)$, we are left with

$$\dot{\mathbf{u}}_s(T)\delta T + \tilde{\mathbf{u}}(T) = \tilde{\mathbf{u}}(0). \tag{40}$$

A similar exercise for (37) gives

$$\tilde{\mathbf{p}}(T) = \tilde{\mathbf{p}}(0), \tag{41}$$

where we have used that $\mathbf{p}_s = 0$ for all times. Moreover, using (23), we have the following expression of the pseudo-energy in (38) in terms of the perturbed limit cycle:

$$\delta E = H(\mathbf{u}_s + \tilde{\mathbf{u}}, \tilde{\mathbf{p}}) \approx \mathbf{f}(\mathbf{u}_s)\cdot\tilde{\mathbf{p}}. \tag{42}$$

By using solutions (35) and $\dot{\mathbf{u}}_s = \mathbf{f}(\mathbf{u}_s) = \mathbf{f}_s$, we may express the three conditions (40), (41), and (42) as

$$\tilde{\mathbf{u}}(0) = \mathbf{f}_s\delta T + M_T\tilde{\mathbf{u}}(0) + N_T\tilde{\mathbf{p}}(0), \tag{43}$$

$$\tilde{\mathbf{p}}(0) = (M_T)^{-T}\tilde{\mathbf{p}}(0), \tag{44}$$

$$\delta E = \mathbf{f}_s\cdot\tilde{\mathbf{p}}(0), \tag{45}$$

where $M_T = M(T)$ and $N_T = N(T)$. Figure 7 shows a sketch of the perturbed limit cycle.

3. Eigenfunction expansion

We now perform a linear transformation of (43)–(45), using the following eigenvalue decomposition:

$$M_T = \sum_{k=1}^{n}\mathbf{e}_k\Lambda_k\mathbf{f}_k^T,$$

where $\{\Lambda_k\}$, $\{\mathbf{e}_k\}$, and $\{\mathbf{f}_k\}$ are, respectively, the Floquet multipliers, the right Floquet vectors, and the left Floquet vectors. The eigenvectors are bi-orthogonal, $\mathbf{f}_k^T\mathbf{e}_l = \delta_{kl}$ and the eigenvalues are ordered as $|\Lambda_1| \geq |\Lambda_2| \geq \ldots \geq |\Lambda_n|$. Note that the first Floquet vector is in the direction of the flow, $\mathbf{e}_1 = \mathbf{f}_s$, and corresponds to the multiplier $\Lambda_1 = 1$.

We may now expand $\tilde{\mathbf{u}}$ in the right Floquet vectors and $\tilde{\mathbf{p}}$ in left vectors, i.e.,

$$\tilde{\mathbf{u}}(0) = \sum_{k=1}^{n} \alpha_k \mathbf{e}_k, \qquad \tilde{\mathbf{p}}(0) = \sum_{k=1}^{n} \beta_k \mathbf{f}_k, \tag{46}$$

and insert into Eqs. (43)–(45),

$$\sum_{k=1}^{n} \alpha_k \mathbf{e}_k = \mathbf{e}_1 \delta T + M_T \sum_{k=1}^{n} \alpha_k \mathbf{e}_k + N_T \sum_{k=1}^{n} \beta_k \mathbf{f}_k, \tag{47}$$

$$\sum_{k=1}^{n} \beta_k \mathbf{f}_k = (M_T)^{-T} \sum_{k=1}^{n} \beta_k \mathbf{f}_k, \tag{48}$$

$$\delta E = \mathbf{e}_1 \sum_{k=1}^{n} \beta_k \mathbf{f}_k = \beta_1. \tag{49}$$

Next, left multiply (47) with $\mathbf{f}_l^T$ and (48) with $\mathbf{e}_l^T$,

$$\alpha_l = \mathbf{f}_l^T \mathbf{e}_1 \delta T + \Lambda_l \alpha_l + \mathbf{f}_l^T N_T \sum_{k=1}^{n} \beta_k \mathbf{f}_k, \tag{50}$$

$$\beta_l = \sum_{k=1}^{n} \mathbf{e}_l^T (M_T)^{-T} \mathbf{f}_k \beta_k = \sum_{k=1}^{n} \left(\mathbf{f}_k^T M_T^{-1} \mathbf{e}_l\right)^T \beta_k = \Lambda_l^{-1} \beta_l. \tag{51}$$

The last expression is satisfied if $\Lambda_l \neq 1$ and $\beta_l = 0$, or if $\beta_l \neq 0$ and $\Lambda_l = 1$. For a limit cycle, only the first multiplier $l = 1$ has a unit value. Therefore, in the space spanned by Floquet vectors, conditions (44) and (45) combined give

$$\beta_l = \begin{cases} \delta E & \text{for} \quad l = 1 \\ 0 & \text{for} \quad l \geq 1. \end{cases}$$

As a consequence, the only non-trivial solution of Eq. (50) reads

$$\alpha_1 = \mathbf{f}_1^T \mathbf{e}_1 \delta T + \alpha_1 + \mathbf{f}_1^T N_T \mathbf{f}_1 \delta E \qquad \rightarrow \qquad \delta T = \left[-\frac{\mathbf{f}_1^T N_T \mathbf{f}_1}{\mathbf{f}_1^T \mathbf{e}_1} \right] \delta E. \tag{52}$$

Using the initial conditions $\tilde{\mathbf{u}}(0) = 0$ and $\tilde{\mathbf{p}}(0) = \mathbf{f}_1$ in (35), we get

$$\tilde{\mathbf{u}}(T) = N_T \mathbf{f}_1,$$

which gives the final expression (3)

$$S = \frac{\partial T}{\partial E} = -\frac{\mathbf{f}_1^T \tilde{\mathbf{u}}(T)}{\mathbf{f}_1^T \mathbf{e}_1}.$$

In Table I the real part of the leading eigenvalue σ_1 is listed for limit cycles of the SL equation with different periods, where it is observed that as S becomes larger, the decay rate (and thus phase diffusion) increases.

It is interesting to note that the factor $\mathbf{f}_1^T / \mathbf{f}_1^T \mathbf{e}_1$ in S also arises in analysis of the response of a linear stable system to harmonic forcing,[30] where it provides a physical insight into where a flow is mostly receptive to forcing. In the current approach, when we consider the full nonlinear stochastic system but with *weak* noise, we observe that the phase diffusive behavior of an oscillator is composed of the same components as the noise amplifying behavior of a linear system. Indeed this is reasonable and intuitive; the assumption of small amplitude disturbances which underlies linear analysis, and the weak noise assumption which underlies the current analysis, are different means of studying small fluctuations around an equilibrium solution (e.g., steady or periodic solutions). Nevertheless, the insight that linear Floquet analysis provides full information of effects of weak noise of a nonlinear system is an important one.

Yet, another connection between hydrodynamic stability theory and weak noise analysis that can be made is the structural sensitivity[18] of a deterministic limit cycle to white noise. Although, such a sensitivity map becomes possible due to the theory presented in Sec. III, it is a sidetrack of the current work and thus only briefly reported in the Appendix.

IV. CONCLUSIONS

Despite the increased complexity due to infinite-dimensionality, we believe that linear evolution operators such as Koopman, Perron-Frobenius, Fokker-Planck, and Chapman-Kolmogorov provide powerful means of analyzing nonlinear systems, since the linearity of the operators enables the formulation of an eigenvalue problem that captures the complete nonlinear system. For a limit cycle, in addition to the frequencies which the flow oscillates with, the time scale which determines the quality factor appears naturally in the spectrum of evolution operators. By assuming the presence of weak noise and employing the theory developed by Gaspard,[5] we elucidated the effects of small amplitude noise on flows with self-sustained oscillations. The effects can be quantified from a local stability analysis, for which there are very well-developed matrix-free tools[31] in the fluids community. Also the method of Dynamic mode decomposition, which is taking its rightful place in the community, may provide information on the effects of noise. However, there is still more work to be done on this method, in particular to generalize it to datasets based on more than one trajectory. One such effort is the recent DMD theory presented in Tu *et al.*,[16] which provides Ritz vectors and values of multiple trajectories.

ACKNOWLEDGMENTS

I like to acknowledge support from the Swedish Research Council (VR-2010-3910). I thank Professor Jan Pralits for discussions and for computing and providing Figure 6.

APPENDIX: CONSEQUENCES OF STRUCTURAL SENSITIVITY

In Luchini, Giannetti, and Pralits[18] the structural sensitivity of a deterministic limit cycle to a generic perturbation was derived. Specifically, they investigated the effect of a structural perturbation $\mathbf{h}(\mathbf{u})$ on the time period, starting from

$$\frac{\partial \tilde{\mathbf{u}}}{\partial t} = A(t)\tilde{\mathbf{u}} + \mathbf{h}(\mathbf{u}), \tag{A1}$$

$$\frac{\partial \tilde{\mathbf{p}}}{\partial t} = -A^T(t)\tilde{\mathbf{p}}. \tag{A2}$$

Assuming a steady forcing proportional to $\mathbf{u}_s$, $\mathbf{h} = C\mathbf{u}_s$, they obtained the following expression:

$$\delta\omega = \frac{\omega}{\mathbf{f}_1^T\mathbf{e}_1}\int \mathbf{f}^T\mathbf{h}(\mathbf{u})dt = \mathrm{trace}(C\bar{S}^T), \tag{A3}$$

where the sensitivity matrix is given by

$$\bar{S} = \frac{\omega}{\mathbf{f}_1^T\mathbf{e}_1}\int \tilde{\mathbf{p}}\mathbf{u}_s^T dt.$$

Various norms of $\bar{S}$ may be used to identify where in space a steady forcing induces a variation of the frequency. We note that if we choose $\mathbf{h} = 2\mathbf{Q}(\mathbf{u})\tilde{\mathbf{p}}$, then Eqs. (A1) and (A2) are Hamilton's equations of motion (33)-(34). We get from (A3),

$$\delta\omega = \frac{2\omega}{\mathbf{f}_1^T\mathbf{e}_1}\int \tilde{\mathbf{p}}^T\mathbf{Q}(\mathbf{u})\tilde{\mathbf{p}}dt = \mathrm{trace}(\bar{Q}S^T),$$

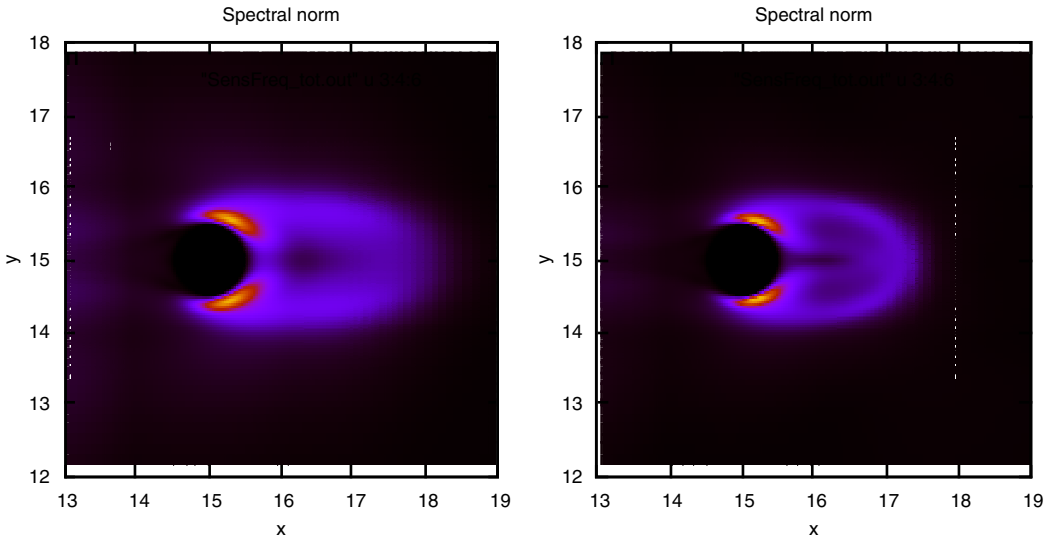

FIG. 8. The spectral norm of $\bar{S}$ for the flow past a circular cylinder at $Re = 60$ (left) and $Re = 100$ (right). The numerical method, resolution, and other parameters are reported in Ref. 18. Figure used with kind permission of Dr. Pralits.

where in the last line we have assumed a constant diffusion matrix $\mathbf{Q} = \bar{Q}$. The sensitivity map reads

$$\bar{S} = \frac{2\omega}{\mathbf{f}_1^T \mathbf{e}_1} \int \tilde{\mathbf{p}} \tilde{\mathbf{p}}^T dt.$$

This sensitivity function defines a spatial map that describes where in space white noise induces a variation in the frequency. Figure 8 shows $\bar{S}$ for $\tilde{\mathbf{p}} = \mathbf{f}_1$ for the flow past a two-dimensional circular cylinder at Reynolds numbers $Re = UD/\nu = 60$ and $Re = 100$ (D is diameter, U free-stream velocity, and ν the kinematic viscosity). We observe that noise sensitivity is localized near the cylinder surface and the recirculation zone. In particular, near the points on the cylinder where the boundary layer separates from the surface (angle around $\theta = 55^\circ$ with respect to the horizontal centerline), noise has the largest impact on the frequency of the periodic vortex shedding.

[1] D. J. Tritton, *Physical Fluid Dynamics*, 2nd ed. (Oxford University Press, Oxford, 1988).
[2] V. Jegadeesan and R. I. Sujith, "Experimental investigation of noise induced triggering in thermoacoustic systems," Proc. Combust. Inst. **34**, 3175 (2013).
[3] T. C. Lieuwen, "Phase drift characteristics of self-excited, combustion-driven oscillations," J. Sound Vib. **242**, 893 (2001).
[4] P. J. Schmid and D. S. Henningson, *Stability and Transition in Shear Flows* (Springer Verlag, New York, 2001).
[5] P. Gaspard, "Trace formula for noisy flows," J. Stat. Phys **106**, 57 (2002).
[6] P. Huerre, "Open shear flow instabilities," in *Perspectives in Fluid Dynamics*, edited by G. K. Batchelor, H. K. Moffatt, and M. G. Worster (Cambridge University Press, Cambridge, UK, 2000), pp. 159–229.
[7] I. Mezić, "Spectral properties of dynamical systems, model reduction and decompositions," Nonlinear Dyn. **41**, 309 (2005).
[8] I. Mezić, "Analysis of fluid flows via spectral properties of the koopman operator," Annu. Rev. Fluid Mech. **45**, 357–378 (2013).
[9] S. Bagheri, "Koopman-mode decomposition of the cylinder wake," J. Fluid Mech. **726**, 596 (2013).
[10] C. W. Rowley, I. Mezić, S. Bagheri, P. Schlatter, and D. S. Henningson, "Spectral analysis of nonlinear flows," J. Fluid Mech. **641**, 115 (2009).
[11] P. J. Schmid, "Dynamic mode decomposition of numerical and experimental data," J. Fluid Mech. **656**, 5 (2010).
[12] P. Schmid, L. Li, M. Juniper, and O. Pust, "Applications of the dynamic mode decomposition," Theo. Comput. Fluid Dyn. **25**, 249 (2011).
[13] P. J. Goulart, A. Wynn, and D. Pearson, "Optimal mode decomposition for high dimensional systems," in *Proceedings of the 51st IEEE Conference on Decision and Control*, Maui, Hawaii (IEEE, 2012). Available at: http://control.ee.ethz.ch/~goularpa/.
[14] C. W. Rowley, I. Mezić, S. Bagheri, P. Schlatter, and D. S. Henningson, "Reduced-order models for flow control: balanced models and koopman modes," in *Seventh IUTAM Symposium on Laminar-Turbulent Transition*, edited by P. Schlatter and D. S. Henningson (Springer, 2009), pp. 43–50.
[15] K. Chen, J. H. Tu, and C. W. Rowley, "Variants of dynamic mode decomposition: Boundary condition, koopman, and fourier analyses," J. Nonlinear Sci. **22**, 887 (2012).

[16] J. Tu, C. W. Rowley, D. M. Luchtenburg, S. L. Brunton, and J. N. Kutz, "On dynamic mode decomposition: Theory and applications," preprint arXiv:1312.0041 (2013).
[17] D. Duke, J. Soria, and D. Honnery, "An error analysis of the dynamic mode decomposition," Exp. Fluids **52**, 529 (2012).
[18] P. Luchini, F. Giannetti, and J. Pralits, "Structural sensitivity of the finite amplitude vortex shedding behind a cicular cylinder," in *IUTAM Symposium on Unsteady Separated Flows and their Control*, edited by M. Braza and K. Hourigan (Springer Science & Business Media, 2009).
[19] J. Guckenheimer and P. Holmes, *Nonlinear Oscillations, Dynamical Systems, and Bifurcations of Vector Fields* (Springer Verlag, New York, 1983).
[20] B. Øksendal, *Stochastic Differential Equations: An Introduction with Applications* (Springer-Verlag, Heidelberg, New York, 2000).
[21] We are assuming that observables are twice differentiable and have a compact support.
[22] B. Koopman, "Hamiltonian systems and transformations in Hilbert space," Proc. Natl. Acad. Sci. U.S.A. **17**, 315 (1931).
[23] G. Froyland, O. Junge, and P. Koltai, "Estimating long-term behavior of flows without trajectory integration: The infinitesimal generator approach," SIAM J. Numer. Anal. **51**, 223 (2013).
[24] In order to simplify the numerical discretization, we Taylor expand the diffusion matrix $Q(\theta, r)$ around $r = \sqrt{\mu}$ and keep only the leading term. The second term in the expansion is $\delta\epsilon \ll \epsilon$ in Eq. (12), and thus comparatively small to the other terms. We impose a periodic boundary condition in θ and a Dirichlet boundary condition in r. Finally, to solve (12), we use a Fourier series in θ direction and finite difference in r direction.
[25] P. Gaspard and S. Tasaki, "Liouvillian dynamics of the Hopf bifurcation," Phys. Rev. E **64**, 056232 (2001).
[26] H. Risken, *The Fokker-Planck Equation: Methods of Solution and Applications* (Springer Verlag, New York, 1996).
[27] P. Cvitanović, "Chapter "Noise"," in *Chaos: Classical and Quantum*, edited by P. Cvitanović, R. Artuso, R. Mainieri, G. Tanner, and G. Vattay (Niels Bohr Institute, Copenhagen, 2013).
[28] M. I. Freidlin and A. D. Wentzell, *Random Perturbations of Dynamical Systems* (Springer Verlag, Berlin, 1984).
[29] P. Gaspard, "The correlation time of mesoscopic chemical clocks," J. Chem. Phys. **117**, 8905 (2002).
[30] J. M. Chomaz, "Global instabilities in spatially developing flows: Non-normality and nonlinearity," Annu. Rev. Fluid Mech. **37**, 357 (2005).
[31] S. Bagheri, E. Akervik, L. Brandt, and D. S. Henningson, "Matrix-free methods for the stability and control of boundary layers," AIAA J. **47**, 1057 (2009).